Circulation Research

ORIGINAL RESEARCH

Small Extracellular Vesicles From Cardiomyocytes Activate Microglia Aggravating HFpEF

Lintong Men*, Qian Wang*, Bowen Ren, Yu Cao, Min Du, Shengqi Huo, Moran Wang, Bingyu Huang, Dewei Peng, Xiaoli He, Lujin Wu, Sheng Li, Cuntai Zhang, Jiaogao Lv, Li Lin*, Junyi Guo*

BACKGROUND: Heart failure with preserved ejection fraction (HFpEF) is increasingly acknowledged as a major public health concern due to its complex pathophysiology, which involves neuroinflammation and sympathetic activation. The crosstalk between the heart and hypothalamic microglia in HFpEF, particularly the role of small extracellular vesicles (sEVs), remains insufficiently explored.

METHODS AND RESULTS: We constructed an HFpEF model in mice by combining a long-term high-fat diet with the nitric oxide synthase inhibitor L-NAME (N[ω]-nitro-L-arginine methyl ester). These mice exhibited microglial activation and hypothalamic inflammation. Microglial depletion with PLX3397 suppressed sympathetic activity and improved cardiac dysfunction in HFpEF. sEVs derived from the myocardium of HFpEF mice induced a proinflammatory M1 phenotype in microglia, leading to hypothalamic inflammation and sympathetic activation. Intraperitoneal injection of the sEV biogenesis inhibitor GW4869 reversed these changes in HFpEF mice. Similar pathological changes were observed in BV2 microglia treated with sEVs isolated from palmitic acid-treated HL-1 cardiomyocytes. Bioinformatic and RT-qPCR analyses revealed a notable upregulation of miR-200c-3p in sEVs derived from both HFpEF myocardial tissue and palmitic acid-treated HL-1 cardiomyocytes, as well as in microglia. A cardiomyocyte-specific miR-200c-3p sponge inhibited microglial activation, hypothalamic inflammation, and sympathetic activation in HFpEF mice. Conversely, a miR-200c-3p mimic exacerbated proinflammatory responses in BV2 cells, while a miR-200c-3p inhibitor prevented the transition to a proinflammatory phenotype. The antiinflammatory protein DUSP1 (dual-specificity phosphatase 1) was validated as a potential downstream target of miR-200c-3p in microglia.

CONCLUSIONS: Our study reveals that HFpEF prompts cardiomyocytes to release sEVs enriched with miR-200c-3p, leading to hypothalamic inflammation and evoking sympathetic outflow, which in turn exacerbates cardiac dysfunction. Focusing on sEV-mediated communication between cardiomyocytes and microglia may offer a new therapeutic approach for HFpEF.

GRAPHIC ABSTRACT: A graphic abstract is available for this article.

Key Words: animals ■ communication ■ heart failure ■ phenotype ■ stroke volume

Heart failure (HF) continues to be a major cause of death globally. Epidemiological evidence has indicated a long-term trend of an overall increase in the prevalence of HF.[1] Notably, this epidemiological pattern is characterized by a shift in subtype distribution. While the incidence of HF with reduced ejection fraction (HFrEF) has begun to stabilize or even decline, HF with preserved ejection fraction (HFpEF) is witnessing a yearly increase in prevalence. Consequently, HFpEF may become the most common form of HF in the future.[2] This trend presents a significant therapeutic challenge, as pharmacological agents that are therapeutically effective for patients with HFrEF do not show similar positive therapeutic effects in patients with HFpEF, leaving a critical unmet need for targeted therapies.[3]

The pathogenesis of HFpEF is complex, with aging, obesity, metabolic disorders, hypertension, and coronary microcirculation disorders being high-risk factors for its

Correspondence to: Li Lin, MD, PhD, Division of Cardiology, Department of Internal Medicine, Tongji Hospital, Tongji Medical College, Huazhong University of Science and Technology, 1095 Jiefang Ave, Wuhan 430030, China, Email linli@tjh.tjmu.edu.cn; or Junyi Guo, MD, PhD, Division of Cardiology, Department of Internal Medicine, Tongji Hospital, Tongji Medical College, Huazhong University of Science and Technology, 1095 Jiefang Ave, Wuhan 430030, China, Email junyiguo@tjh.tjmu.edu.cn
*L. Men, Q. Wang, L. Li, and J. Guo contributed equally.
Supplemental Material is available at https://www.ahajournals.org/doi/suppl/10.1161/CIRCRESAHA.125.327765.

Circulation Research is available at www.ahajournals.org/journal/res

Novelty and Significance

What Is Known?

- Patients suffering from heart failure with preserved ejection fraction (HFpEF) exhibit systemic and cardiac sympathetic activation.
- In heart failure with reduced ejection fraction, microglial activation drives a chronic neuroinflammatory state, which in turn induces sympathetic excitation and contributes to cardiac dysfunction.
- Small extracellular vesicles act as crucial intercellular transporters, delivering functional cargoes such as proteins, microRNAs, and DNAs, thereby playing significant roles in both physiological and pathological processes.

What New Information Does This Article Contribute?

- Hypothalamic microglia ablation attenuates the systemic and cardiac sympathetic overactivity observed in HFpEF mice.
- Cardiac-derived small extracellular vesicles from HFpEF mice induce microglial activation and hypothalamic inflammation.
- Mechanistically, miR-200c-3p encapsulated in cardiomyocyte-derived small extracellular vesicles promotes proinflammatory polarization of hypothalamic microglia, with DUSP1 (dual-specificity phosphatase 1) identified as a potential downstream target.

HFpEF is projected to become the predominant form of heart failure in the coming years, yet its pathogenesis remains incompletely understood. Neuroinflammation driven by microglial activation might play a role in HFpEF progression. We demonstrate that in HFpEF, cardiac-derived small extracellular vesicles transport miR-200c-3p to hypothalamic microglia. This suppresses the antiinflammatory regulator DUSP1 and triggers hypothalamic inflammation and sympathetic overactivation, which then worsens cardiac function, thereby creating a self-reinforcing heart-brain axis. These results identify microglial activation as a modifiable determinant of disease progression and reveal miR-200c-3p as a promising intervention point.

Nonstandard Abbreviations and Acronyms

DUSP1	dual specificity phosphatase 1
HF	heart failure
HFpEF	heart failure with preserved ejection fraction
HFrEF	heart failure with reduced ejection fraction
LV	left ventricular
miRNA	microRNA
PA	palmitic acid
sEV	small extracellular vesicle
TH	tyrosine hydroxylase

onset.[2] Recently, neuroinflammation has been considered to play an important role in the development of HF.[4] Specifically, neuroinflammation contributes to sympathetic overexcitation by disrupting autonomic balance through the activation of key brain regions, particularly hypothalamic and brainstem nuclei.[5] As resident immune cells in the central nervous system, microglia play essential roles in hypothalamic inflammation development and homeostatic maintenance.[6,7] Upon activation by pathological stimuli, microglia release proinflammatory cytokines, which initiate and sustain hypothalamic inflammation. This neuroinflammatory milieu enhances neuronal activity in sympathetic regulatory nuclei, leading to increased sympathetic outflow.[8,9] Consequently, elevated sympathetic drive manifests as tachycardia, vasoconstriction, and increased cardiac afterload, establishing a vicious cycle that exacerbates cardiovascular dysfunction.[4,10] Previous studies have shown that patients with HFpEF exhibit systemic and cardiac sympathetic activation.[11,12] However, the exact contribution of microglial activation to hypothalamic neuroinflammation and the pathogenesis of HFpEF remains unclear.

Interorgan communication is increasingly recognized as important in disease progression. Small extracellular vesicles (sEVs) are heterogeneous membrane-enclosed vesicles that are secreted by virtually all cells. The lipids, peptides, proteins, and nucleic acids they carry play key roles in physiological and pathological processes.[13,14] Studies have indicated that in HFrEF, sEVs can penetrate the blood-brain barrier, and the microRNAs they transport can amplify the inflammatory response within the rostral ventrolateral medulla, enhancing sympathetic nerve activation and exacerbating cardiac damage.[15,16] The effect of sEVs on microglial activation and hypothalamic inflammation in HFpEF, however, has not been investigated.

In this study, we hypothesized that in HFpEF, cardiac-derived sEVs transport specific miRNAs (microRNAs) to the brain. These miRNAs induce microglial activation, leading to hypothalamic neuroinflammation and evoking sympathetic excitation, which in turn exacerbates cardiac dysfunction. Both male and female mice can be successfully induced to develop HFpEF phenotypes using the

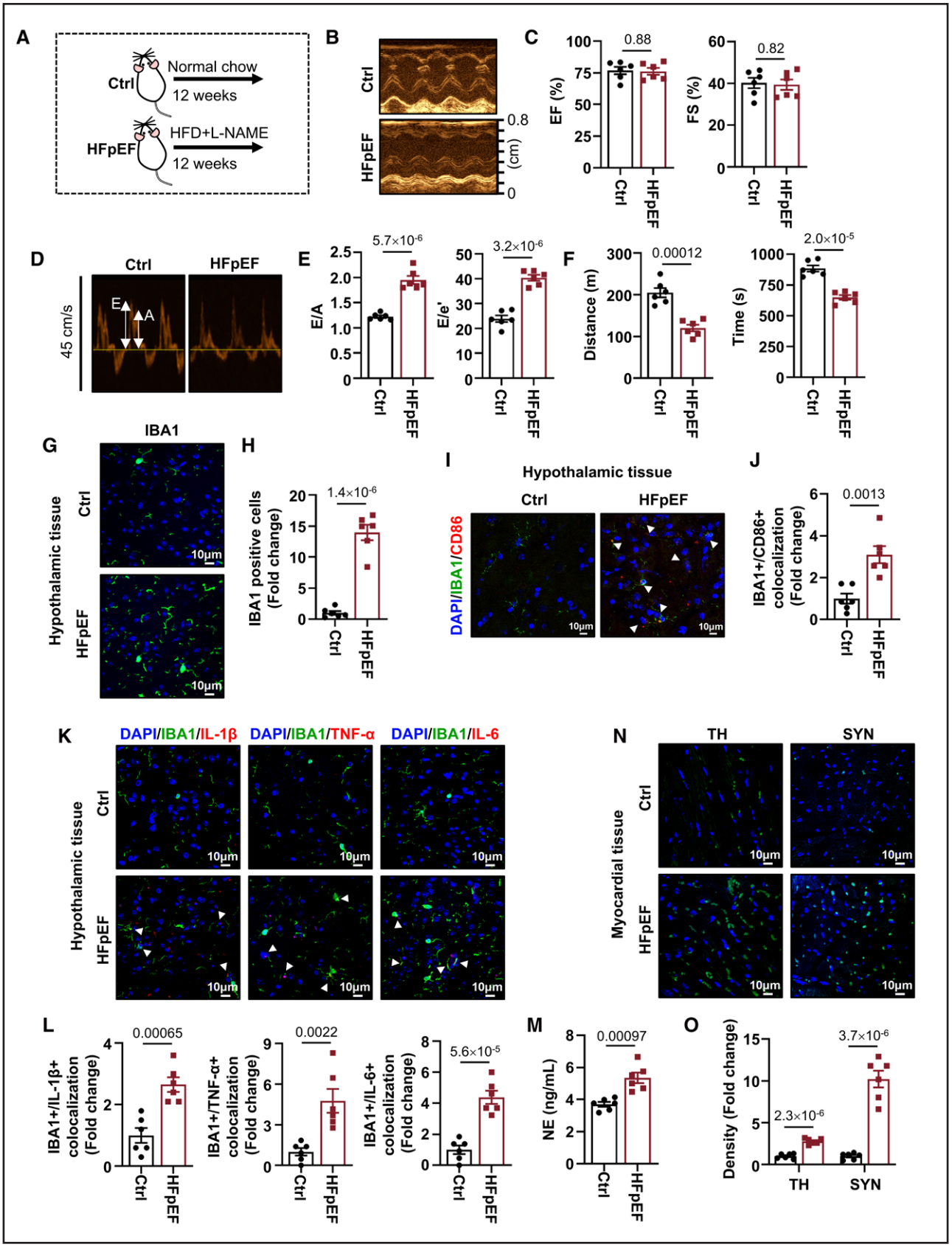

Figure 1. Heart failure with preserved ejection fraction (HFpEF) mice exhibited microglial activation, hypothalamic inflammation and increased sympathetic drive.

A, Schematic of the 2-hit strategy. **B** and **C**, Representative echocardiographic images and statistical analysis of left ventricular (*Continued*)

well-established 2-hit model. Using this model, combined with molecular, cellular, and functional analyses, this study aimed to test our hypothesis and elucidate a novel heart-brain signaling axis in HFpEF pathophysiology.

METHODS

Data Availability

The microRNA sequencing data generated during this study will be available in the public repository GEO under accession number GSE334160. The data supporting the findings are available from the corresponding author upon reasonable request. Expanded protocols, reagents, antibodies, primers, and additional details are provided in the Supplemental Material.

Experimental Animals

All animal experiments were approved by the Animal Care and Use Committee of Tongji Medical College, Huazhong University of Science and Technology (TJH-202305030). HFpEF was induced in C57BL/6J mice (8–10 weeks old) by a high-fat diet (60% kcal) plus L-NAME (N[ω]-nitro-L-arginine methyl ester; 0.5 g/L in drinking water) for 12 weeks (male) or 8 weeks (female). For microglial depletion, PLX3397 (290 ppm in the diet) was given for the final 2 weeks. For sEV inhibition, GW4869 (2.5 mg/kg, IP) was administered every 3 days throughout the model period. For cardiomyocyte-specific miR-200c-3p sponge expression, adeno-associated virus serotype 9 carrying the sponge or a negative control under the cTnT (cardiac troponin T) promoter was injected via the tail vein 2 to 4 weeks before model induction. For sEV transfer, male mice were injected with 100 μg of myocardial sEVs via the tail vein every 5 days (3 injections total). Detailed methods for echocardiography, hemodynamics, glucose/insulin tolerance tests, blood pressure, and treadmill exercise are provided in the Supplemental Material.

sEV Isolation and Characterization

Myocardial- and HL-1 cell-derived sEVs were isolated by differential ultracentrifugation and characterized by TEM, flow nanoanalysis, and Western blot. DiR-labeled sEVs were injected via the tail vein for in vivo uptake, and PKH26-labeled sEVs were used for in vitro uptake in BV2 microglia. Detailed methods are described in the Supplemental Material.

Cell Culture and In Vitro Treatments

HL-1 cardiomyocytes and BV2 microglia were cultured in DMEM with 10% FBS. HL-1 cells were treated with PA (100 μM, 24 hours). The conditioned medium or its derived sEVs were applied to BV2 cells. miRNA gain/loss of function were achieved by transfection with a miR-200c-3p mimic or inhibitor using Lipofectamine 2000. Detailed methods are described in the Supplemental Material.

Western Blot and qRT-PCR

Protein lysates were resolved by SDS-PAGE, transferred to PVDF membranes, probed with specific antibodies, and detected by chemiluminescence. Total RNA was reverse-transcribed and analyzed by qRT-PCR using SYBR Green, with Rn18s for mRNA or U6 for miRNA as internal controls. Detailed methods are described in the Supplemental Material.

Immunofluorescence and Immunohistochemistry

Paraffin sections were stained with primary antibodies followed by fluorophore-conjugated or HRP-conjugated secondary antibodies. Fluorescence in situ hybridization combined with immunofluorescence was performed using custom miR-200c-3p probes. Detailed methods are described in the Supplemental Material.

Statistical Analysis

Normality was assessed by the Shapiro-Wilk test. Two-group comparisons were performed using an unpaired *t* test or the Mann-Whitney *U* test, whereas multiple-group comparisons were performed using 1-way ANOVA with Tukey post hoc testing or the Kruskal-Wallis test with Dunn post hoc testing. Data are presented as mean±SEM. A $P<0.05$ was considered significant. Exact *P* values and n are provided in the figure legends. Detailed statistical methods are provided in the Supplemental Material.

RESULTS

HFpEF Mice Exhibited Microglial Activation, Hypothalamic Inflammation, and Increased Sympathetic Drive

HFpEF frequently coexists with comorbidities such as obesity, diabetes, hypertension, and so on. To model this clinical spectrum, we used an established 2-hit strategy combining sustained metabolic (high-fat diet) and hemodynamic stressors (L-NAME in drinking water) to recapitulate the key phenotypes of HFpEF. After 12 weeks, mice developed obesity, glucose intolerance,

Figure 1 Continued. ejection fraction (EF) and fractional shortening (FS; n=6 per group). **D** and **E**, Representative echocardiographic images and statistical data of diastolic function (E/A and E/e′; n=6 per group). **F**, Exercise time and distance in the mouse treadmill exhaustion test (n=6 per group). **G** and **H**, Representative immunofluorescence images of IBA1 in hypothalamic tissue and the number of IBA1-positive cells (scale bar=10 μm, n=6 per group, 3 random areas per hypothalamus). **I** and **J**, Representative immunofluorescence images and quantitative analysis of IBA1 colocalized with CD86 in hypothalamic tissue (scale bar=10 μm, n=6 per group, 3 random areas per hypothalamus). **K** and **L**, Representative immunofluorescence images and quantitative analysis of IBA1 colocalized with IL-1β, TNF-α, and IL-6 in hypothalamic tissue (scale bar=10 μm, n=6 per group, 3 random areas per hypothalamus). **M**, Quantitative data of serum norepinephrine (NE) levels (n=6 per group). **N** and **O**, Representative immunofluorescence images and quantitative analysis of tyrosine hydroxylase (TH) or synaptophysin (SYN) in myocardial tissue (scale bar=10 μm, n=6 per group, 3 random areas per heart). Each point represents a mouse. For panel **M**, 2 to 3 technical replicates were performed per sample and averaged before analysis. Data are shown as mean±SEM and analyzed using an unpaired *t* test (**C**, **E**, **F**, **H**, **J**, **L**, **M**, and **O**). Exact *P* values are specified in the corresponding figures.

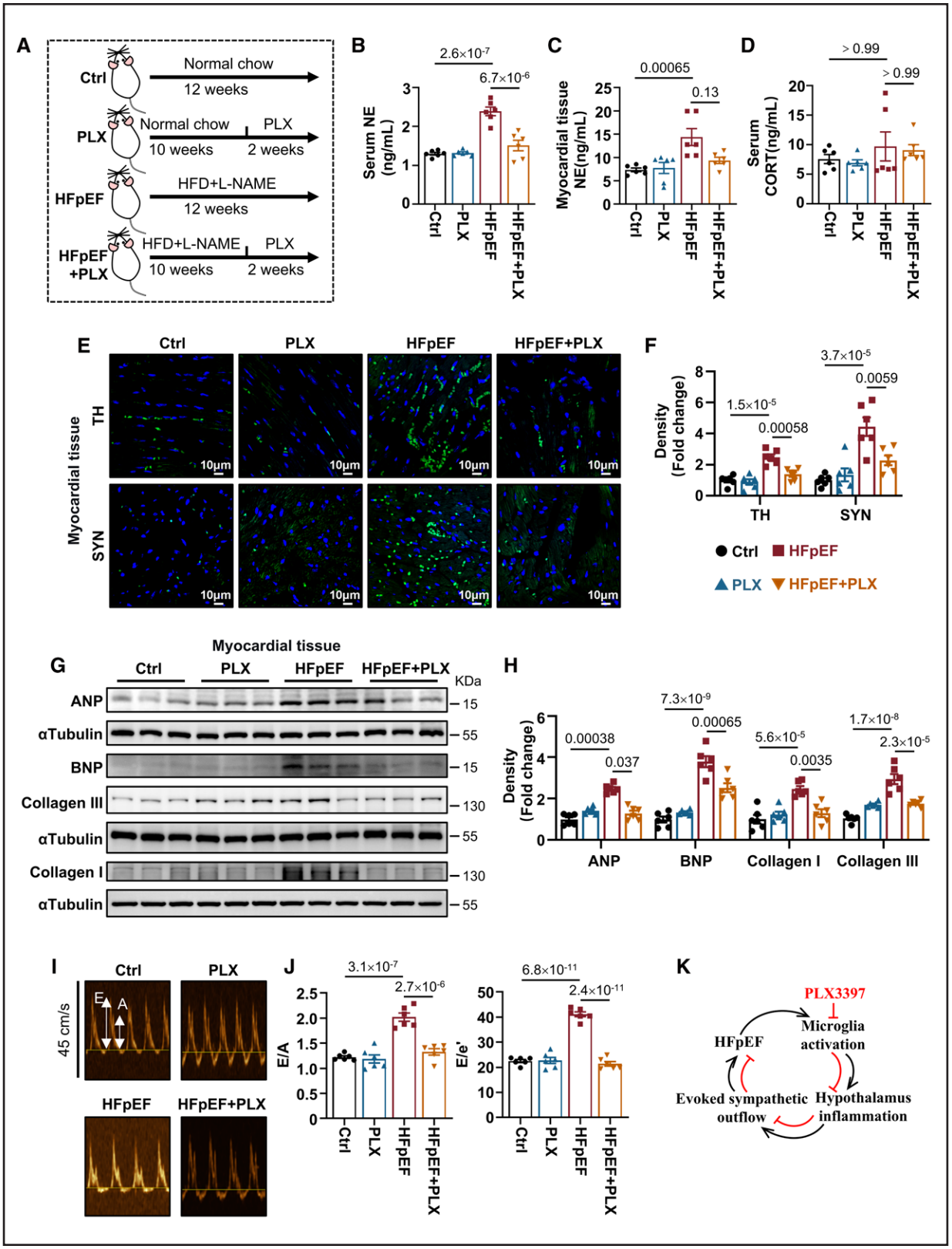

Figure 2. PLX3397-mediated microglia depletion attenuates sympathetic excitation and restores cardiac function in heart failure with preserved ejection fraction (HFpEF) mice.

A, Schematic diagram of the experimental timeline. Mice were treated with the 2-hit strategy for 12 weeks, and PLX3397 (PLX, 290 ppm) was added to the diet during the last 2 weeks (n=6 per group). **B**, Quantitative data of serum norepinephrine (NE) level (n=6 per group). **C**, Quantitative data of myocardial tissue NE levels (n=6 per group). **D**, Quantitative data of serum corticosterone (CORT) levels (n=6 per group). **E** and **F**, Representative immunofluorescence images and quantitative analysis of tyrosine hydroxylase (TH) or synaptophysin (*Continued*)

insulin resistance, hypercholesterolemia, and hypertension (Figure 1A; Figure S1A through S1E). Echocardiography revealed a restrictive ventricular filling pattern and diastolic dysfunction in HFpEF mice, indicated by an elevation in E/A and E/e′ ratios despite preserved LV ejection fraction (Figure 1B through 1E; Figure S1F). This was along with markedly reduced exercise capacity (Figure 1F). Structural remodeling in HFpEF mice was evidenced by increased left ventricular (LV) mass and posterior wall thickness at end-diastole (Figure S1G). Cardiac catheterization showed that systolic contractility (dp/dt_{max}) was preserved, where as diastolic dysfunction (dp/dt_{min}) was evident in HFpEF mice, which correlated positively with elevated E/e′ ratios (Figure S1H and S1I). These changes were consistent with an elevated heart weight-to-tibial length ratio and histologically verified cardiac hypertrophy (Figure S1J through S1M). Moreover, cardiac Nos2 expression and the phospho-IRE1α/IRE1α ratio were significantly elevated in the HFpEF model (Figure S1N and S1O). In aggregate, 2-hit-treated mice exhibited the key pathological features of HFpEF.

Immunofluorescence staining revealed a significant increase in IBA1-positive cells within the hypothalamus of HFpEF mice (Figure 1G and 1H). Furthermore, these microglia exhibited a proinflammatory phenotypic shift, characterized by elevated secretion of cytokines, including IL-1β, TNF-α, and IL-6, contributing to hypothalamic inflammation (Figure 1I through 1L; Figure S2A and S2B), while the amygdala and cerebral cortex showed no obvious inflammation (Figure S2C through S2F). This neuroinflammatory state was accompanied by elevated serum levels of norepinephrine (Figure 1M). Consistent with enhanced sympathetic drive, the myocardial expression of the sympathetic markers tyrosine hydroxylase (TH) and synaptophysin was also increased in HFpEF mice (Figure 1N and 1O; Figure S2G and S2H). Collectively, these findings indicate that HFpEF is associated with hypothalamic microglial activation, neuroinflammation, and a consequent increase in sympathetic outflow (Figure S2I).

PLX3397-Mediated Microglial Depletion Attenuates Sympathetic Excitation and Ameliorates Cardiac Dysfunction in HFpEF Mice

To investigate the role of microglial activation in sympathetic nerve excitation and cardiac dysfunction in HFpEF, we used PLX3397, a CSF1R (colony-stimulating factor 1 receptor) inhibitor capable of crossing the blood-brain barrier and depleting microglia within the central nervous system. Mice subjected to the 2-hit strategy for 12 weeks received a PLX3397-supplemented (290 ppm) high-fat diet during the final 2 weeks (Figure 2A). This treatment significantly reduced the number of hypothalamic microglia but had no significant effect on macrophages in myocardial tissue (Figure S3A and S3B).

PLX3397 substantially reduced myocardial tissue and serum norepinephrine levels, concurrently diminishing the 2-hit strategy-induced increases in the sympathetic markers synaptophysin and TH. However, the PLX3397-supplemented diet did not affect serum corticosterone levels (Figure 2B through 2F).

Regarding the metabolic and hemodynamic profile, PLX3397 failed to suppress 2-hit-induced obesity (Figure S3C) but improved glucose intolerance, insulin resistance, and serum cholesterol levels (Figure S3D through S3F), and prevented the development of hypertension in this model (Figure S3G).

The expression levels of myocardial hypertrophy and fibrosis markers, including ANP (atrial natriuretic peptide), BNP (brain natriuretic peptide), Collagen I, and Collagen III, were significantly elevated in 2-hit-treated mice, but PLX3397 inhibited these changes (Figure 2G and 2H). Echocardiography showed that PLX3397 significantly ameliorated the 2-hit model-induced diastolic dysfunction, as indicated by improved E/A and E/e′ ratios, without altering LV systolic function (Figure 2I and 2J; Figure S4A through S4C). This was corroborated by decreased LV mass and posterior wall thickness at end-diastole (Figure S4D). PLX3397 also enhanced exercise tolerance (Figure S4E). In addition, the ratios of lung wet/dry weight and heart weight normalized to tibial length were increased in 2-hit-treated mice, but these increases were reversed by the PLX3397-supplemented diet (Figure S4F and S4G). This finding was further confirmed by histological analyses showing decreased interstitial fibrosis and cardiomyocyte cross-sectional area (Figure S4H and S4I). Collectively, these data demonstrate that pharmacological inhibition of microglial activation reduces sympathetic nervous system activity and rescues cardiac dysfunction in HFpEF mice (Figure 2K).

Consistent with observations in male mice, female mice subjected to the 2-hit strategy exhibited increased body weight, a restrictive ventricular filling pattern, and diastolic dysfunction. Although PLX3397 treatment did

Figure 2 Continued. (SYN) in myocardial tissue (scale bar=10 μm, n=6 per group, 3 random areas per heart). **G** and **H**, Western blot analysis and quantification of atrial natriuretic peptide (ANP), brain natriuretic peptide (BNP), Collagen I, and Collagen III in cardiac tissue from mice with or without the PLX3397-supplemented diet after the 2-hit strategy (n=6 per group). **I** and **J**, Representative echocardiographic images and statistical data of diastolic function (E/A and E/e′; n=6 per group). **K**, Schematic illustration. The relative protein levels were determined by comparing them with the first sample in the control group. Each point represents a mouse. For panels **B**, **C**, **D**, and **H**, 2 to 3 technical replicates were performed per sample and averaged before analysis. Data are shown as mean±SEM and analyzed using 1-way ANOVA with Tukey multiple comparisons test (**B**, **F**, BNP, Collagen I and Collagen III in **H**, and **J**) or the Kruskal-Wallis test (**C**, **D**, and ANP in **H**). Exact *P* values are specified in the corresponding figures.

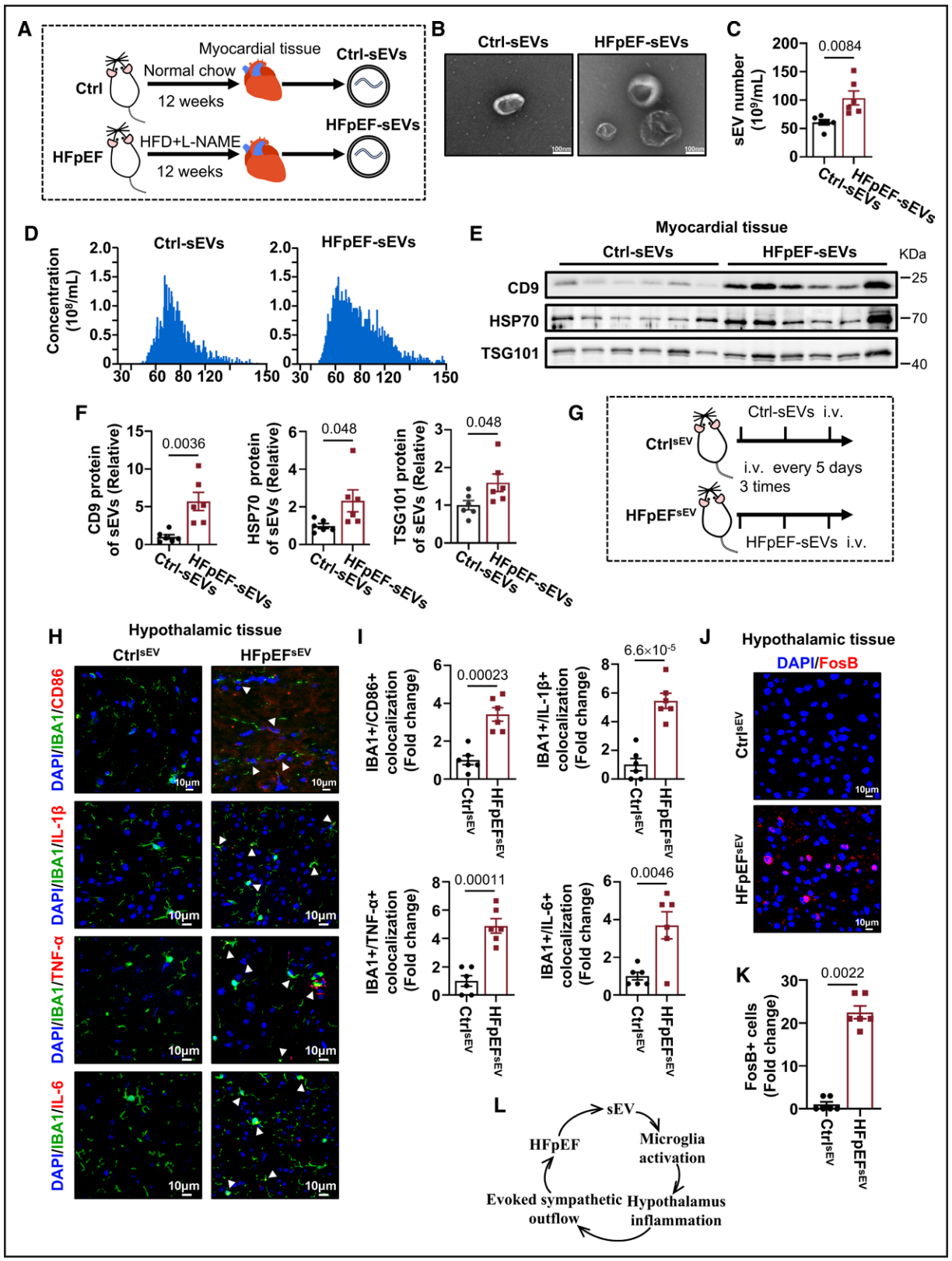

Figure 3. Cardiac-derived small extracellular vesicles (sEVs) from heart failure with preserved ejection fraction (HFpEF) mice induce microglial activation and hypothalamic inflammation.

A, Schematic representation of myocardial sEV extraction and grouping. Small extracellular vesicles were extracted from the myocardial tissue of control mice and labeled as Ctrl-sEVs. Small extracellular vesicles were extracted from the myocardial tissue of HFpEF mice and labeled as HFpEF-sEVs. **B**, Morphology of sEVs secreted by myocardial tissue from control and 2-hit-treated mice observed by transmission electron microscopy. Scale bar=200 nm. **C**, The number of sEVs (n=6 per group). **D**, Particle size distribution measured by nanoparticle (*Continued*)

not attenuate body weight gain (Figure S5A), it significantly improved diastolic function, as evidenced by a reduced E/e′ ratio, decreased LV mass, and reduced posterior wall thickness at end-diastole. Ejection fraction and fractional shortening remained unchanged (Figure S5B through S5J).

Cardiac-Derived sEVs From HFpEF Mice Induce Microglial Activation and Hypothalamic Inflammation

We have shown that suppressing microglial activation ameliorates HFpEF, pointing to a brain-to-heart regulatory axis. To explore the potential reverse communication, we next examined a heart-to-brain pathway. Based on evidence that cardiac-derived sEVs contribute to neuroinflammation in HFrEF, we hypothesized that sEVs from HFpEF hearts might similarly exacerbate hypothalamic microglial activation and the associated pathological crosstalk.

sEVs were isolated from the myocardial tissue of control mice (Ctrl-sEVs) or HFpEF mice (HFpEF-sEVs; Figure 3A). Although sEV morphology and size were similar between groups, HFpEF mice exhibited markedly increased sEV secretion (Figure 3B through 3F). Subsequent in vivo imaging demonstrated that intravenously administered sEVs were taken up by the brain, with kinetic analysis revealing their distribution in the cerebral cortex, amygdala, and hypothalamus. Notably, sEVs colocalized with microglia specifically within the hypothalamus (Figure S6A through S6C).

Next, to investigate the effects of myocardial sEVs on hypothalamic inflammation and microglial activation, we injected equal amounts of sEVs (100 μg) every 5 days into C57BL/6 mice (Figure 3G). Compared with the Ctrl^{sEV} group, HFpEF^{sEV} mice exhibited a shift of microglia to the proinflammatory phenotype, as well as an increased secretion of the inflammatory cytokines IL-1β, TNF-α, and IL-6 (Figure 3H and 3I; Figure S6D through S6F). In addition, as an indicator of sympathetic neuronal activity, immunofluorescence staining showed a markedly higher count of FosB-positive cells in HFpEF^{sEV} group (Figure 3J and 3K).

The mice in the HFpEF^{sEV} group exhibited increased random blood glucose and blood pressure, unchanged serum cholesterol, and exercise intolerance (Figure S7A through S7D). Echocardiography indicated no significant alterations in cardiac function in the HFpEF^{sEV} group compared with the Ctrl^{sEV} group (Figure S7E through S7J). In addition, the lung wet/dry weight ratio and heart weight-to-tibial length ratio showed no change in HFpEF^{sEV} group (Figure S7K and S7L). ELISA and immunofluorescence staining indicated sympathetic activation in the myocardial tissue (Figure S7M through S7O). Although histological staining revealed no significant changes in cardiomyocyte cross-sectional area or fibrosis, Western blot analysis confirmed elevated levels of HF markers and collagen accumulation in the model group (Figure S7P through S7S). Collectively, sEVs derived from the myocardium of HFpEF mice induced microglial polarization and hypothalamic inflammation (Figure 3L).

In vitro, conditioned medium from HL-1 cardiomyocytes stimulated with palmitic acid (PA) activated BV2 microglia and promoted M1 polarization (Figure S8A through S8C). sEVs were isolated from the conditioned medium of control (CON-sEVs) and PA-stimulated HL-1 cells (PA-sEVs). These vesicles exhibited a characteristic bilayer morphology and a diameter of 30 to 150 nm. PA-sEVs were more abundant than CON-sEVs and were internalized by BV2 microglia within 12 hours (Figure S8D through S8G). Compared with CON-sEVs, PA-sEVs significantly upregulated the mRNA and protein levels of proinflammatory cytokines (IL-1β, IL-6, and TNF-α) in BV2 cells and concurrently drove a shift toward the M1 phenotype (Figure S8H through S8J).

Inhibition of sEV Biogenesis Ameliorates Microglial Activation, Hypothalamic Inflammation, and Cardiac Dysfunction in HFpEF Mice

To assess the role of sEVs in heart-brain communication in vivo, we administered the sEV biogenesis inhibitor GW4869 to 2-hit model mice (Figure 4A). After 12 weeks, nanoflow cytometry analysis confirmed a reduction in myocardial sEV levels (Figure 4B). This inhibition attenuated hypothalamic microglial activation and inflammation (Figure 4C and 4D; Figure S9A through S9C), which subsequently reduced sympathetic activity, as evidenced by fewer FosB-positive cells, lower serum norepinephrine, and decreased cardiac TH density (Figure 4E and 4F; Figure S9D through S9F). Concomitantly,

Figure 3 Continued. tracking analysis (NTA). **E** and **F**, Western blot analysis and quantification of sEV markers CD9, HSP70, and TSG101 in sEVs derived from the myocardial tissue of control and 2-hit-treated mice (n=6 per group). **G**, Schematic representation of the experimental timeline. Myocardial sEVs were extracted and injected into healthy mice via the tail vein every 5 days. **H** and **I**, Representative immunofluorescence images and quantitative analysis of IBA1 colocalized with CD86, IL-1β, TNF-α, and IL-6 in hypothalamic tissue (scale bar=10 μm, n=6 per group, 3 random areas per hypothalamus). **J** and **K**, Representative images of FosB staining and quantitative analysis of FosB-positive cells in hypothalamic tissue sections (scale bar=10 μm, n=6 per group, 3 random areas per hypothalamus). **L**, Schematic illustration. The relative protein levels were determined by comparing them with the first sample in the control group. Each point represents a mouse. Data are shown as mean±SEM and analyzed using an unpaired *t* test (**C**, **F**, and **I**) or as medians with interquartile ranges and analyzed using the Mann-Whitney *U* test (K). Exact *P* values are specified in the corresponding figures.

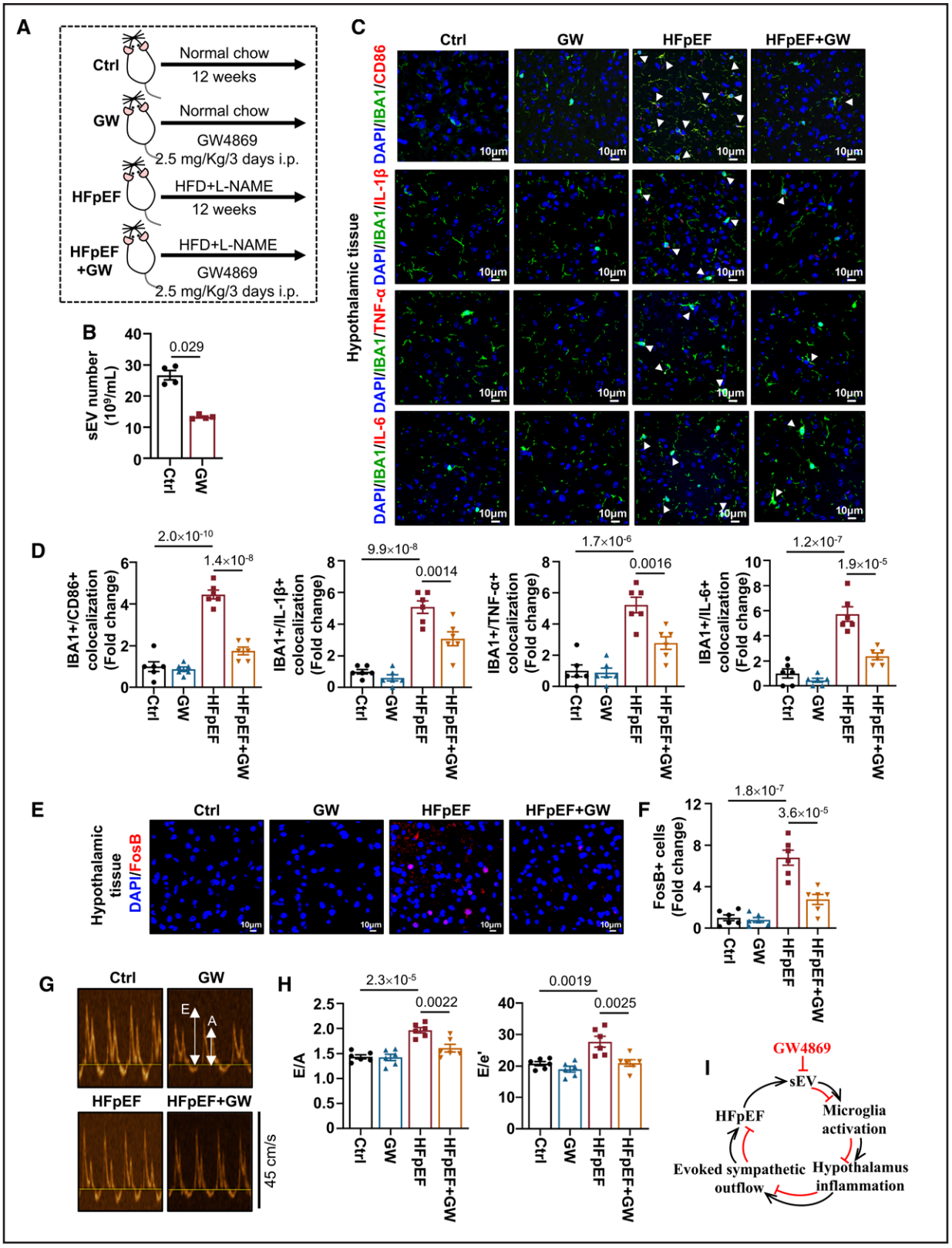

Figure 4. Inhibition of small extracellular vesicle (sEV) biogenesis ameliorates microglial activation, hypothalamic inflammation, and cardiac dysfunction in heart failure with preserved ejection fraction (HFpEF) mice.

A, Schematic of the experimental timeline. Mice treated with the 2-hit strategy received intraperitoneal injections of GW4869 (GW, 2.5 mg/kg) every 3 days for 12 weeks. **B**, The number of sEVs isolated from myocardial tissue (n=3 per group). **C** and **D**, Representative immunofluorescence images and quantitative analysis of IBA1 colocalized with CD86, IL-1β, TNF-α, and IL-6 in hypothalamic tissue (scale bar=10 μm, n=6 per group, 3 random areas per hypothalamus). **E** and **F**, Representative images of FosB staining and quantitative analysis of (*Continued*)

GW4869 improved systemic metabolism, lowered blood pressure, and enhanced exercise tolerance (Figure S10A through S10F). Crucially, it ameliorated key HFpEF cardiac phenotypes, including diastolic dysfunction, ventricular remodeling, and pathological hypertrophy, without affecting systolic function (Figure 4G and 4H; Figure S10G through S10N). These data underscore a critical pathological role for sEV-mediated heart-brain communication in HFpEF (Figure 4I).

In addition, in female mice subjected to an 8-week HFpEF-inducing diet, concurrent GW4869 treatment did not affect body weight or systolic function but significantly ameliorated cardiac diastolic dysfunction (Figure S11A through S11J).

miR-200c-3p in HL-1-Derived sEVs Drives BV2 Microglial Activation

The internal cargo of sEVs is fundamental to their role in intercellular communication. To identify miRNAs that might mediate the pathological effects of cardiac sEVs in HFpEF, we performed miRNA microarray analysis on myocardial tissue from control and 2-hit model mice. This revealed 28 miRNAs with the most significant differential expression (15 upregulated, 13 downregulated; Figure 5A). Subsequent quantitative PCR validation in BV2 microglia stimulated with cardiomyocyte-conditioned medium identified miR-200c-3p as markedly upregulated (Figure 5B).

To trace the origin of this increase, we measured miR-200c-3p levels in PA-stimulated HL-1 cardiomyocytes. Both the mature miR-200c-3p and its primary transcript (pri-miR-200c) were significantly elevated (Figure 5C). Importantly, when sEV biogenesis was inhibited by GW4869 during PA stimulation, intracellular miR-200c-3p levels increased further (Figure 5D; Figure S12), indicating that GW4869 treatment blocked its secretion via sEVs, leading to its accumulation in cardiomyocytes. Consistent with sEV-mediated transfer, miR-200c-3p was also highly expressed in BV2 cells treated with sEVs from PA-stimulated cardiomyocytes (PA-sEVs), as well as in the hypothalamic tissue of 2-hit model mice and mice injected with HFpEF-sEVs, without a corresponding increase in pri-miRNA levels (Figure 5E through 5G). While these findings implicate cardiac sEVs in elevating miR-200c-3p in microglia, its direct functional role required confirmation.

Transfection of a miR-200c-3p mimic into BV2 cells significantly elevated the levels of proinflammatory cytokines (IL-1β, IL-6, and TNF-α) and promoted a shift toward the M1 phenotype (Figure 5H). Conversely, a miR-200c-3p inhibitor attenuated the inflammatory response induced by PA-sEV treatment (Figure 5I). Together, these results establish that miR-200c-3p, packaged into sEVs from the HFpEF myocardium, is a key molecular inducer of proinflammatory microglial activation.

Cardiac-Specific Inhibition of miR-200c-3p Attenuates Hypothalamic Inflammation and Ameliorates HFpEF Phenotypes

To further validate the pathological involvement of miR-200c-3p in cardiomyocyte-derived sEVs contributing to hypothalamic inflammation post-HFpEF, we used a cardiac-specific adeno-associated virus serotype 9 vector. This vector was driven by the cTnT promoter to express either a miR-200c-3p sponge or a negative control sequence (sponge). After 4 weeks of adeno-associated virus serotype 9 injection, mice underwent the 2-hit protocol for 12 weeks (Figure 6A). Western blot analysis showed that the miR-200c-3p mimic had no influence on hypertrophy markers in HL-1 cardiomyocytes (Figure S13A and S13B). A microRNA-specific probe was designed, and fluorescence in situ hybridization on paraffin-embedded tissue sections revealed a significant decrease in microRNA expression in the myocardial tissue and hypothalamic tissue following viral injection (Figure S13C and S13D). This was also corroborated by quantitative real-time PCR analysis (Figure 6B and 6C). The miR-200c-3p sponge significantly alleviated hypothalamic inflammation, as evidenced by decreased proinflammatory cytokines (IL-1β, TNF-α, IL-6) and reduced M1 polarization (Figure 6D and 6E; Figure S14A through S14C). It also reduced the number of FosB-positive cells and TH density in the hypothalamus (Figure 6F and 6G; Figure S14D and S14E), restored serum and myocardial norepinephrine levels (Figure S14F and S14G), and decreased myocardial TH expression (Figure S14H and S14I).

In HFpEF mice, the cardiac-specific miR-200c-3p sponge had no effect on body weight or systolic function but significantly improved glucose and cholesterol metabolism, reduced blood pressure, restored exercise capacity, and attenuated LV mass and posterior wall thickness at end-diastole, indicating amelioration of diastolic dysfunction (Figure 6H and 6I; Figure S15A through S15J). In addition, the miR-200c-3p sponge reduced the lung wet/dry ratio and prevented pathological cardiac hypertrophy (Figure S15K through S15N). Collectively, these data suggest that miR-200c-3p derived from cardiomyocytes may play a pivotal role in regulating microglial activation in HFpEF mice (Figure 6J).

Figure 4 Continued. FosB-positive cells in hypothalamic tissue sections (scale bar=10 μm, n=6 per group, 3 random areas per hypothalamus). **G** and **H**, Representative echocardiographic images and statistical data of diastolic function (E/A and E/e′; n=6 per group). **I**, Schematic illustration. Each point represents a mouse. Data are shown as mean±SEM and analyzed using the Mann-Whitney *U* test (**B**) or 1-way ANOVA with Tukey multiple comparisons test (**D**, **F**, and **H**). Exact *P* values are specified in the corresponding figures.

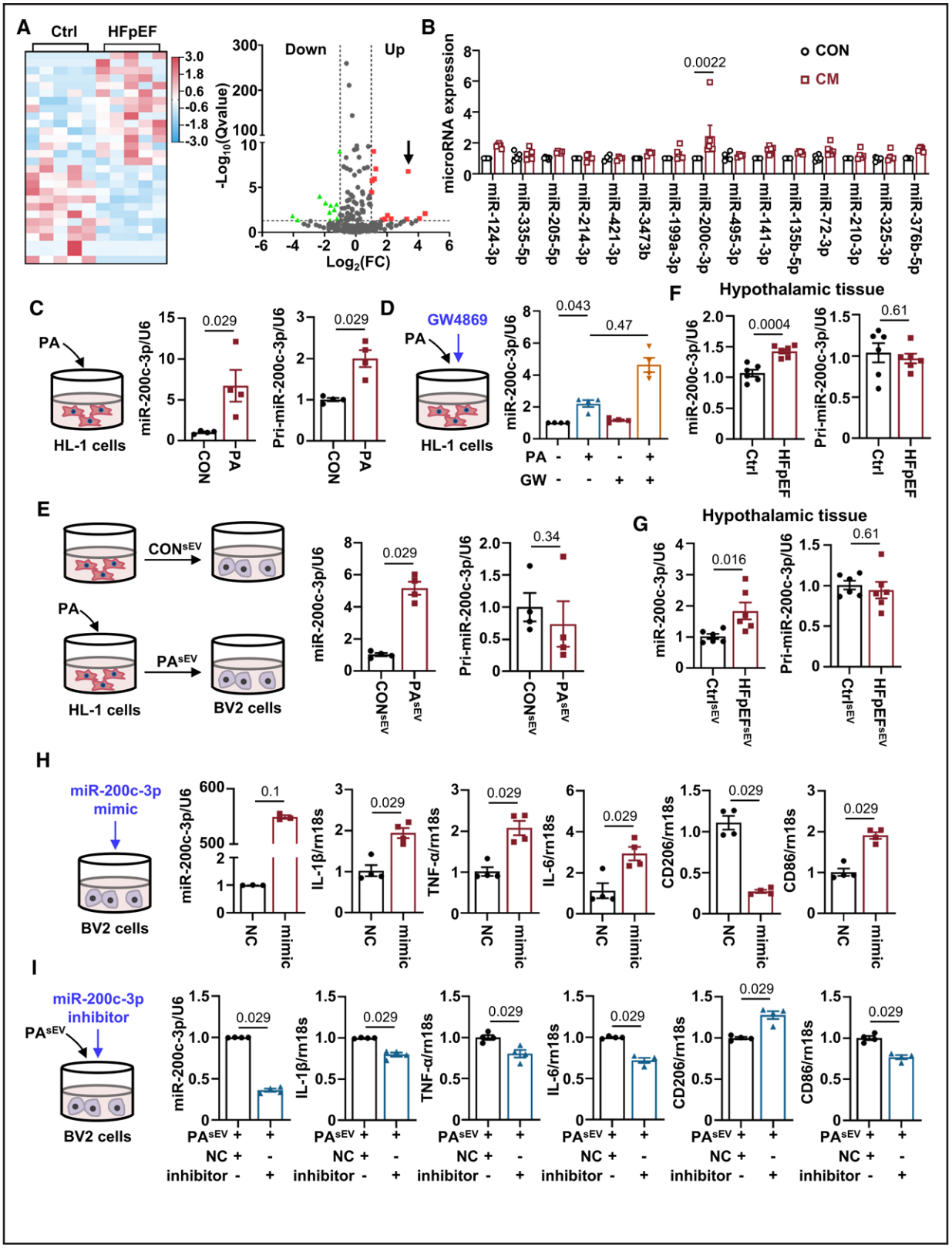

Figure 5. miR-200c-3p in HL-1-derived small extracellular vesicles (sEVs) drives BV2 microglial activation.
A, Heat map and volcano plot of microRNA (miRNA) expression. miRNA PCR array and differential miRNA analysis of myocardial tissue sEVs from normal diet mice and 2-hit-treated mice. The arrow indicates miR-200c-3p. **B**, Expression of upregulated miRNAs in BV2 cells stimulated by HL-1-conditioned medium (n=4–6 per group). **C**, The expression levels of mature miR-200c-3p and pri-miR-200c in HL-1 cells after palmitic acid (PA) stimulation (n=4 per group). **D**, The expression analysis of miR-200c-3p in HL-1 cells stimulated with PA for 24 hours with or without GW4869 (n=4 per group). **E**, Expression levels of mature and precursor forms of miR-200c in BV2 cells after stimulation with (*Continued*)

In female mice, adeno-associated virus serotype 9 was injected 2 weeks before initiation of a 6-week HFpEF-inducing diet. The miR-200c-3p sponge did not affect body weight gain (Figure S16A). Echocardiography revealed that the miR-200c-3p sponge had no effect on systolic function but significantly ameliorated diastolic dysfunction (Figure S16B through S16J).

DUSP1 as a Potential Target of miR-200c-3p: Preliminary Evidence in Microglial Activation

Next, we searched for potential target genes of miR-200c-3p using databases such as TargetScan, ENCORI, and miRDB. Through these resources, we pinpointed DUSP1 (dual-specificity protein phosphatase 1) as a prospective target gene of miR-200c-3p (Figure 7A). The dual-luciferase reporter assay confirmed that miR-200c-3p targets the 3′-UTR of DUSP1 and inhibits its translation (Figure 7B; Figure S17A). Subsequent experiments reinforced the regulatory relationship between miR-200c-3p and DUSP1. Initially, the miR-200c-3p mimic suppressed the expression of DUSP1 protein and mRNA (Figure 7C and 7D; Figure S17B). The polyclonal BV2 cell pool with CRISPR-Cas9-edited mutations in the DUSP1 3′-UTR showed a significant attenuation of the proinflammatory response induced by the miR-200c-3p mimic, compared with the wild-type control pool (Figure 7E; Figure S17C). Consistently, BV2 cells were treated with a miR-200c-3p inhibitor and PA-sEVs. DUSP1 protein levels decreased with PA-sEV treatment alone but increased after transfection with the miR-200c-3p inhibitor (Figure S17D through S17G). Furthermore, we performed Western blot analysis to detect DUSP1 protein and mRNA levels in hypothalamic tissue in vivo. The DUSP1 level in the hypothalamic tissue of mice injected with HFpEF-sEVs via the tail vein decreased compared with the Ctrl^{sEV} group (Figure 7F through 7H). GW4869 increased DUSP1 expression in the hypothalamic tissue of 2-hit-treated mice (Figure 7I through 7K). Similarly, HFpEF mice receiving the miR-200c-3p sponge exhibited increased hypothalamic DUSP1 expression compared with those receiving the negative control sponge (Figure 7L through 7N). Next, cotransfection of a plasmid containing the DUSP1 gene sequence with the miR-200c-3p mimic significantly restored the inhibitory effect on proinflammatory phenotype polarization of microglia induced by miR-200c-3p overexpression (Figure 7O). Finally, immunofluorescence showed that the miR-200c-3p sponge increased the colocalization of IBA1 and DUSP1 compared with the negative control sponge (Figure S17H and S17I). These data suggest that miR-200c-3p promoted the proinflammatory phenotype shift by targeting DUSP1 in BV2 cells.

DISCUSSION

In the present study, we established a mouse model of HFpEF using a 2-hit strategy, which recapitulates key metabolic and hemodynamic features of human HFpEF. Using this model, we identified hypothalamic microglial activation as a critical node in HFpEF progression and established cardiomyocyte-derived sEVs as a key contributor to this activation. The amount of sEVs released from cardiomyocytes was increased in the setting of cardiac diastolic dysfunction. These sEVs could traverse the blood-brain barrier, activate microglia, and promote hypothalamic inflammation, leading to sympathetic nervous system overactivation and exacerbating cardiac dysfunction. These results elucidate heart-brain interactions in HFpEF and suggest sEV-mediated microglial activation as a potential therapeutic target.

The hypothalamus serves as a critical central regulator of autonomic and metabolic homeostasis, with key nuclei controlling sympathetic outflow located within this region.[6,17] As resident immune cells of the CNS, microglia continuously monitor the brain microenvironment and respond to pathological stimuli.[18–20] Growing evidence indicates that microglial activation contributes significantly to hypothalamic inflammation, which in turn disrupts metabolic balance and promotes sympathetic excitation—a mechanism implicated in HFrEF.[21,22] Patients with HFpEF also exhibit systemic and cardiac sympathetic activation.[11,12] Besides, recent neuroimaging studies have reported associations between hypothalamic gliosis and major HFpEF risk factors, suggesting a plausible clinical relevance of central inflammatory changes to HFpEF.[23] However, the role of microglia in HFpEF remains poorly defined. In this study, we established a murine model of HFpEF by combining a high-fat diet with L-NAME administration in drinking water,

Figure 5 Continued. CON-sEVs or PA-sEVs for 24 hours (n=4 per group). **F**, Expression levels of mature miR-200c-3p and pri-miR-200c in hypothalamic tissue (n=6 per group). **G**, Small extracellular vesicles were extracted from 2-hit-treated mice and injected into normal mice via the tail vein, followed by analysis of mature and precursor miR-200c levels in hypothalamic tissue (n=6 per group). **H**, BV2 cells were transfected with miR-200c-3p mimic or negative control (NC) for 24 hours, followed by mRNA expression analysis of IL-1β, IL-6, TNF-α, CD86, and CD206 (n=3–4 per group). **I**, BV2 cells were stimulated with PA-sEVs and cotransfected with a miR-200c-3p inhibitor for 24 hours. The mRNA expression levels of IL-1β, IL-6, TNF-α, CD86, and CD206 were then measured (n=4 per group). The relative mRNA levels were determined by comparing them with the average expression in the control group. Data points represent individual mice for in vivo panels (**F** and **G**) or independent experiments for in vitro assays (**B**, **C**, **D**, **E**, **H**, and **I**). For panels (**B** through **I**), 2 to 3 technical replicates were performed per sample and averaged before analysis. Data are shown as mean±SEM and analyzed using an unpaired *t* test (**F** and **G**), the Mann-Whitney *U* test (**B**, **C**, **E**, **H**, and **I**), or the Kruskal-Wallis test (**D**). Exact *P* values are specified in the corresponding figures. HFpEF indicates heart failure with preserved ejection fraction.

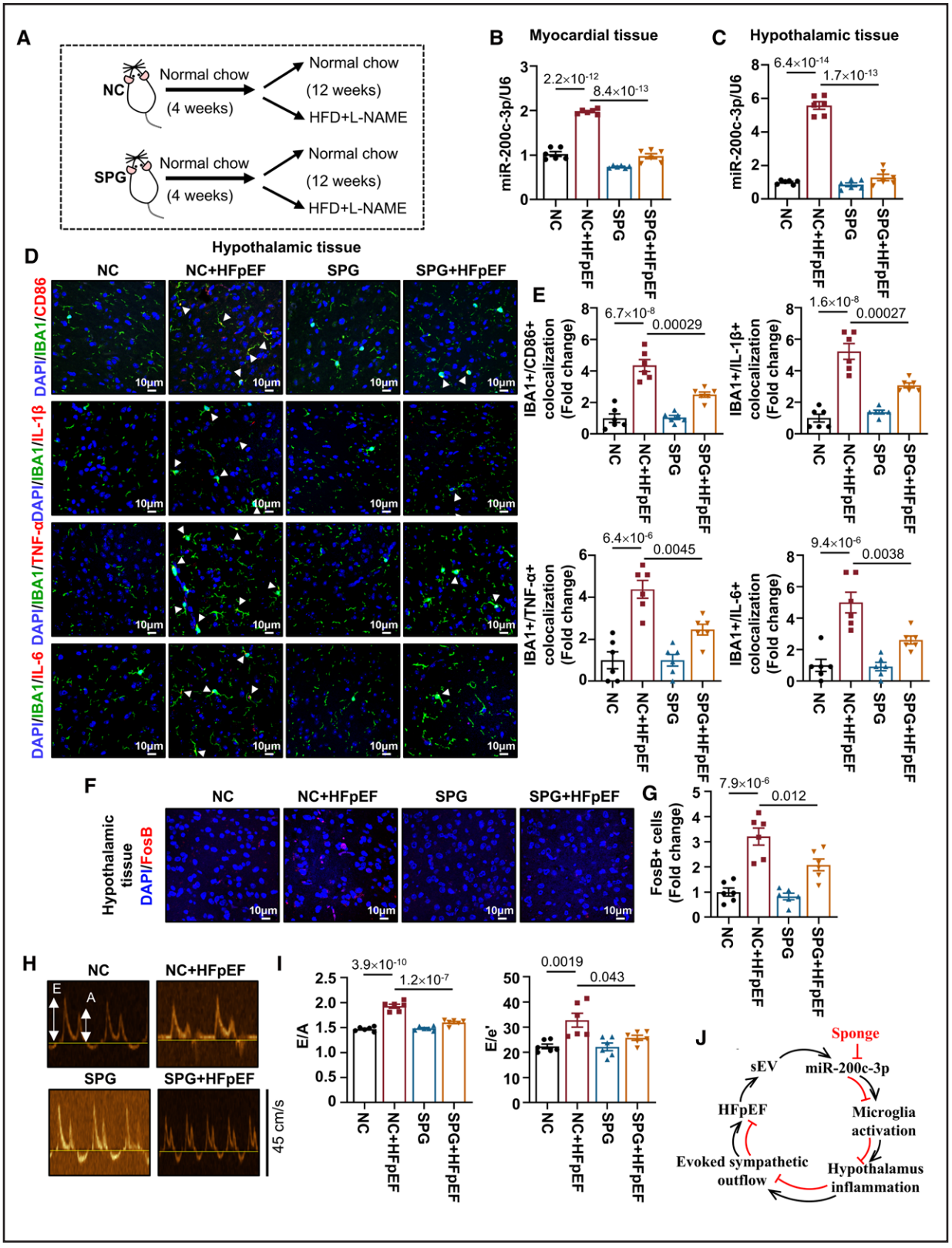

Figure 6. Cardiac-specific inhibition of miR-200c-3p attenuates hypothalamic inflammation and ameliorates heart failure with preserved ejection fraction (HFpEF) phenotypes.

A, Schematic of the experimental timeline. The miR-200c-3p sponge (SPG) and the negative control (NC) sponge were delivered by AAV9 vectors with the cTnT promoter. Four weeks after AAV9 injection, the 2-hit strategy was applied. **B**, Expression level of miR-200c-3p in myocardial tissue (n=6 per group). **C**, Expression level of miR-200c-3p in hypothalamic tissue (n=6 per group). **D** and **E**, Representative immunofluorescence images and quantitative analysis of IBA1 colocalized with CD86, IL-1β, TNF-α, and IL-6 in hypothalamic tissue (*Continued*)

recapitulating major clinical features of HFpEF, including diastolic dysfunction and metabolic disturbances. Interestingly, the present work reveals for the first time that HFpEF mice also exhibit hypothalamic microglial activation and neuroinflammation, suggesting a previously underappreciated role of the central nervous system in HFpEF pathogenesis.

To probe the functional contribution of microglia, we used PLX3397, a second-generation CSF1R inhibitor that selectively depletes microglia.[24] Oral administration of PLX3397 effectively attenuated both sympathetic overactivity and diastolic impairment in HFpEF mice, supporting an important role for microglia-driven hypothalamic inflammation in disease progression. Notably, microglia depletion also ameliorated HFpEF-related systemic comorbidities, including hypertension, insulin resistance, and hyperlipidemia. This finding aligns with a recent clinical study linking hypothalamic gliosis to hypertension and metabolic disorders,[23] connecting hypothalamic inflammation to metabolic syndrome.[25] Our findings not only elucidate a novel brain-heart axis in HFpEF but also highlight microglial modulation as a potential therapeutic strategy.

Previous studies have shown that cardiomyocytes alter the quantity or size of secreted sEVs under various pathological stimuli.[26,27] In the present study, although the 2-hit HFpEF challenge did not alter the size of cardiac-derived sEVs, it significantly increased the number of secreted particles. Cardiomyocyte-derived sEVs are systemically distributed and can mediate intercellular communication in distant organs, including adipose tissue, the lung, and the kidney.[28–31] Our tracing experiments demonstrated that while the majority of fluorescently labeled sEVs were cleared by the liver and spleen, a subset successfully crossed the blood-brain barrier and localized to brain tissue.

The heart and brain share multiple pathophysiological pathways and are jointly influenced by common cardiovascular risk factors such as hypertension, diabetes, and dyslipidemia.[32] These 2 organs communicate via multiple feedback mechanisms, among which sEVs serve as key signaling intermediaries enabling bidirectional interaction. On the one hand, brain injuries, including stroke and Alzheimer's disease, can induce cardiac dysfunction through circulating extracellular vesicles.[33,34] On the other hand, cardiac injury, such as myocardial infarction, modulates neuronal activity via vesicle-mediated signaling.[35] In this study, we observed that sEVs derived from the hearts of HFpEF mice induced microglial activation and hypothalamic inflammation, revealing a heart-to-brain regulatory axis. Notably, although mice receiving HFpEF-sEVs did not develop overt echocardiographic or structural cardiac changes at the observed time point, molecular analysis revealed a significant upregulation of key HF and fibrosis markers. This suggests that sEV-induced neuroinflammation is sufficient to initiate an early, subclinical molecular stress response in the heart, providing a plausible mechanistic link to disease progression. This observation aligns with the multi-hit paradigm of HFpEF, where no single insult is sufficient to produce the full phenotype. We propose that hypothalamic inflammation functions not as a solitary trigger but as a critical integrator and amplifier within this framework. Peripheral comorbidities such as hypertension and metabolic stress may promote sEV release from the heart, which activates hypothalamic microglia and sympathetic drive. This neural response then feeds back to worsen cardiac pathology, creating a vicious cycle that accelerates disease progression. Supporting this model, pharmacological inhibition of sEV biogenesis with GW4869 mitigated hypothalamic neuroinflammation, restored autonomic balance, and alleviated cardiac dysfunction. These results confirm the functional significance of this sEV-mediated heart-brain communication pathway in HFpEF.

sEVs are enriched with noncoding RNAs, particularly miRNAs, whose composition varies substantially across cell types.[36,37] By combining in vivo and in vitro experimentation with bioinformatic analysis, we identified miR-200c-3p as being upregulated in injured cardiomyocytes and shuttled via cardiac sEVs to microglia, where it promoted a shift toward an M1 proinflammatory phenotype and induced hypothalamic inflammation. Furthermore, in vivo inhibition of miR-200c-3p in cardiomyocytes using an adeno-associated virus under a troponin-specific promoter reversed microglial activation, alleviated hypothalamic inflammation, reduced sympathetic outflow, and ultimately improved diastolic function in HFpEF mice. Further analysis revealed that miR-200c-3p acts, at least in part, by targeting DUSP1, a key negative regulator of MAPK (mitogen-activated protein kinase) signaling.[38,39] Its suppression provides a plausible mechanism for the amplification and perpetuation of neuroinflammation in the disease.

Several limitations should be acknowledged in this study. Although we have now included female mice, the treatment duration in females was shorter than in that male mice, though it remains within the reported range for HFpEF phenotype development in female C57BL/6J mice. Longer-term female studies are warranted to confirm intervention efficacy and evaluate potential sex

Figure 6 Continued. (scale bar=10 µm, n=6 per group, 3 random areas per hypothalamus). **F** and **G**, Representative images of FosB staining and quantitative analysis of FosB-positive cells in hypothalamic tissue sections (scale bar=10 µm, n=6 per group, 3 random areas per hypothalamus). **H** and **I**, Representative echocardiographic images and statistical data of diastolic function (E/A and E/e′; n=6 per group). **J**, Schematic illustration. Each point represents a mouse. Data are shown as mean±SEM and analyzed using 1-way ANOVA with Tukey multiple comparisons test (**B**, **C**, **E**, **G**, **I**, and **J**). Exact *P* values are specified in the corresponding figures.

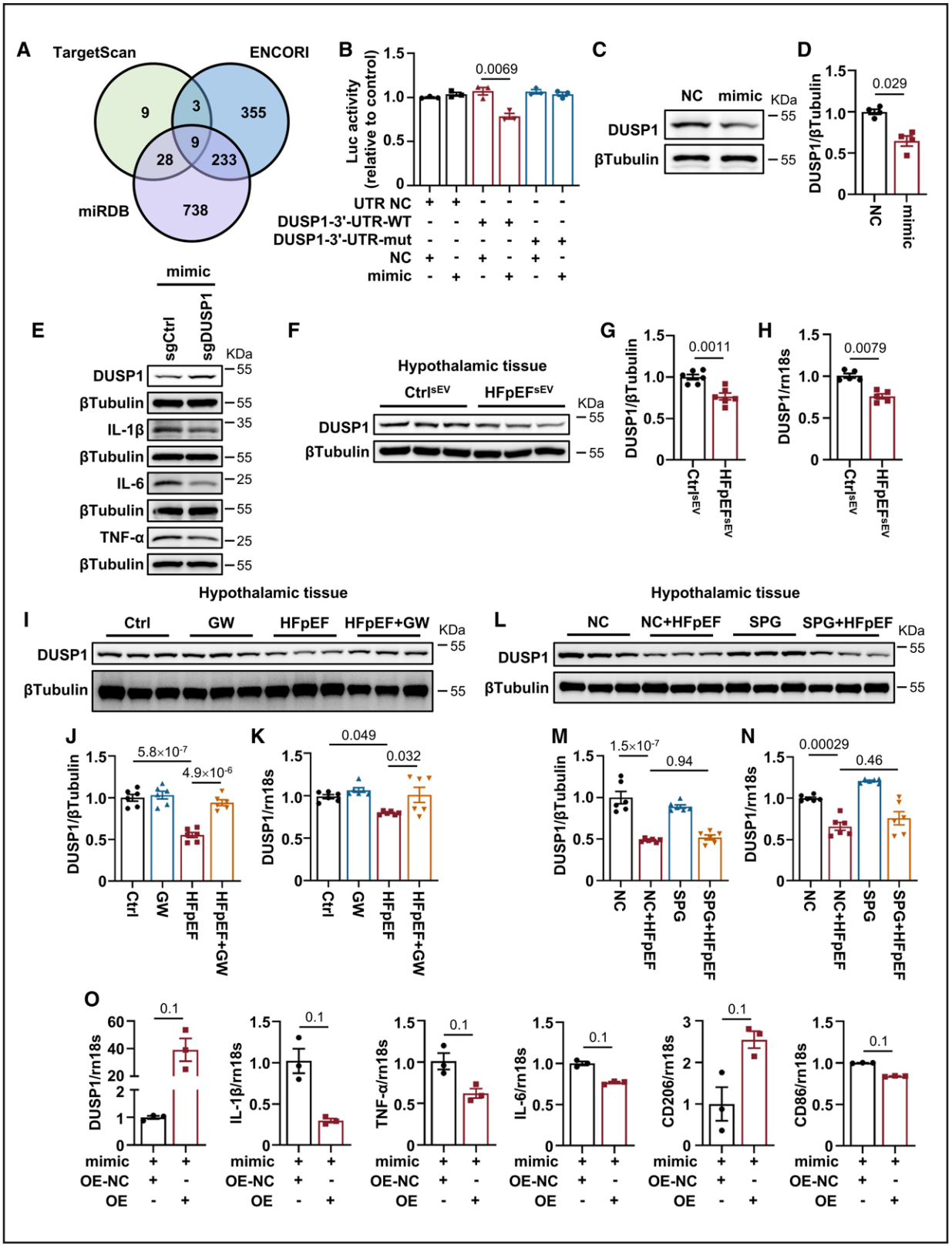

Figure 7. DUSP1 (dual-specificity phosphatase 1) as a potential target of miR-200c-3p: preliminary evidence in microglial activation.

A, Venn diagram comparing 3 target gene prediction algorithms, including TargetScan, miRDB, and ENCORI. **B**, Luciferase activity assay confirmed that DUSP1 microRNA (mRNA) directly binds to miR-200c-3p in HEK-293T cells (n=3 per group). **C** and **D**, After transfecting BV2 cells with miR-200c-3p mimic, DUSP1 protein levels were measured and quantified (n=4 per group). **E**, Protein levels of DUSP1, IL-1β, TNF-α, and IL-6 were measured in BV2 cells. Mutating the miR-200c-3p binding site in the DUSP1 3′-UTR was performed using the (*Continued*)

Figure 7 Continued. CRISPR/Cas9 gene-editing system (sgDUSP1; n=3–4 per group). **F** through **H**, Myocardial tissue sEVs were extracted from 2-hit-treated mice and injected into normal mice via the tail vein. Protein and mRNA expression levels of DUSP1 in hypothalamic tissue were measured (n=5–6 per group). **I** through **K**, Protein and mRNA expression levels of DUSP1 in hypothalamic tissue (n=6 per group). **L** through **N**, Protein and mRNA expression levels of DUSP1 in hypothalamic tissue (n=6 per group). **O**, BV2 cells were cotransfected with a DUSP1 overexpression (OE)/empty (OE-NC) construct and a miR-200c-3p mimic for 24 hours. The mRNA expression levels of DUSP1, IL-1β, IL-6, TNF-α, CD86, and CD206 were measured in BV2 cells stimulated with the miR-200c-3p mimic (n=3 per group). The relative protein levels were determined by comparing them with the first sample in the control group. The relative mRNA levels were determined by comparing them with the average expression in the control group. Data points represent individual mice for in vivo panels (**G**, **H**, **J**, **K**, **M**, and **N**) or independent experiments for in vitro assays (**B**, **D**, and **O**). For panels **B**, **H**, **K**, **N**, and **O**, 2 to 3 technical replicates were performed per sample and averaged before analysis. Data are shown as mean±SEM and analyzed using 1-way ANOVA with Tukey multiple comparisons test (**J**, **M**, and **N**), the Kruskal-Wallis test (**K**), an unpaired *t* test (**G**), the Mann-Whitney *U* test (**D**, **H**, and **O**), or Welch *t* test (**B**). Exact *P* values are specified in the corresponding figures.

differences.[40] Moreover, direct evidence of hypothalamic inflammation in patients with HFpEF is lacking. These limitations necessitate cautious interpretation of our findings and highlight the need for studies in alternative models and human subjects. Second, while systemic sEV injection models physiological distribution, more targeted approaches (eg, stereotactic delivery) would strengthen causality. Third, the use of HL-1 atrial cells may not fully mirror ventricular pathology. Finally, our mechanistic investigation focused on miR-200c-3p with DUSP1 as one of its potential targets, which represents only 1 component of a likely multifactorial process. Exploration of other sEV cargo and in vivo DUSP1 rescue studies are needed to fully elucidate this communication axis.

In conclusion, this study delineates a bidirectional heart-brain signaling loop in HFpEF wherein cardiac-derived sEVs deliver miR-200c-3p to hypothalamic microglia, suppressing DUSP1 and driving neuroinflammation and sympathetic excitation, which in turn exacerbate cardiac dysfunction. These results position central microglial activation as a modifiable determinant of HFpEF progression and identify miR-200c-3p as a potential target for therapeutic intervention.

ARTICLE INFORMATION

Received October 21, 2025; revision received July 7, 2026; accepted July 10, 2026.

Affiliations

Division of Cardiology, Tongji Hospital, Tongji Medical College (L.M., B.R., Y.C., M.D., S.H., M.W., D.P., X.H., L.W., S.L., J.L., L.L., J.G.), Key Laboratory of Vascular Aging, Ministry of Education, Tongji Hospital, Tongji Medical College (L.M., Q.W., B.R., Y.C., M.D., S.H., M.W., D.P., X.H., S.L., C.Z., J.L., L.L., J.G.), and Department of Geriatrics, Tongji Hospital, Tongji Medical College (Q.W., C.Z.), Huazhong University of Science and Technology, Wuhan, China.Peking Union Medical College Hospital, Chinese Academy of Medical Sciences (CAMS) and Peking Union Medical College (PUMC), Beijing, China (B.H.).

Acknowledgments

The authors express their gratitude to every member of our laboratory for their insightful discussions and contributions to this work.

Author Contributions

L. Men conceptualized the study, performed experiments and data analysis, created the figures, and drafted the manuscript. Q. Wang assisted in study design and experiments, and participated in manuscript revision. B. Ren, Y. Cao, M. Du, S. Huo, and M. Wang contributed to animal model establishment. B. Huang provided technical support and resources for bioinformatic analyses. D. Peng and X. He contributed to data interpretation and discussion. L. Wu, S. Li, and C. Zhang contributed to data interpretation and manuscript revision. J. Lv, L. Lin, and J. Guo supervised the project, provided funding, and approved the final version of the manuscript. All authors read and approved the final manuscript.

Sources of Funding

This work was supported by grants from the National Natural Science Foundation of China (grants 82070396, 81974032, and 82370362) and the Natural Science Foundation of Tongji Hospital (grant 2022B11).

Disclosures

None.

Supplemental Material

Supplemental Materials and Methods
Tables S1–S3
Figures S1–S17
Major Resources Table
Uncropped Western Blots
References 41,42

REFERENCES

1. Kapelios CJ, Shahim B, Lund LH, Savarese G. Epidemiology, clinical characteristics and cause-specific outcomes in heart failure with preserved ejection fraction. *Card Fail Rev.* 2023;9:e14. doi: 10.15420/cfr.2023.03
2. Campbell P, Rutten FH, Lee MM, Hawkins NM, Petrie MC. Heart failure with preserved ejection fraction: everything the clinician needs to know. *Lancet.* 2024;403:1083–1092. doi: 10.1016/S0140-6736(23)02756-3
3. Omote K, Verbrugge FH, Borlaug BA. Heart failure with preserved ejection fraction: mechanisms and treatment strategies. *Annu Rev Med.* 2022;73:321–337. doi: 10.1146/annurev-med-042220-022745
4. Díaz HS, Toledo C, Andrade DC, Marcus NJ, Del Rio R. Neuroinflammation in heart failure: new insights for an old disease. *J Physiol.* 2020;598:33–59. doi: 10.1113/JP278864
5. Francis J, Chu Y, Johnson AK, Weiss RM, Felder RB. Acute myocardial infarction induces hypothalamic cytokine synthesis. *Am J Physiol Heart Circ Physiol.* 2004;286:H2264–H2271. doi: 10.1152/ajpheart.01072.2003
6. Rosin JM, Kurrasch DM. Emerging roles for hypothalamic microglia as regulators of physiological homeostasis. *Front Neuroendocrinol.* 2019;54:100748. doi: 10.1016/j.yfrne.2019.100748
7. Tahmasebi F, Barati S. The role of microglial depletion approaches in pathological condition of CNS. *Cell Mol Neurobiol.* 2023;43:2459–2471. doi: 10.1007/s10571-023-01326-8
8. Wolf SA, Boddeke HW, Kettenmann H. Microglia in physiology and disease. *Annu Rev Physiol.* 2017;79:619–643. doi: 10.1146/annurev-physiol-022516-034406
9. Borst K, Schwabenland M, Prinz M. Microglia metabolism in health and disease. *Neurochem Int.* 2019;130:104331. doi: 10.1016/j.neuint.2018.11.006
10. Andrade DC, Toledo C, Díaz HS, Lucero C, Arce-Álvarez A, Oliveira LM, Takakura AC, Moreira TS, Schultz HD, Marcus NJ, et al. Ablation of brainstem C1 neurons improves cardiac function in volume overload heart failure. *Clin Sci (Lond).* 2019;133:393–405. doi: 10.1042/CS20180589
11. Kaye DM, Nanayakkara S, Wang B, Shihata W, Marques FZ, Esler M, Lambert G, Mariani J. Characterization of cardiac sympathetic nervous system and inflammatory activation in HFpEF patients. *JACC Basic Transl Sci.* 2022;7:116–127. doi: 10.1016/j.jacbts.2021.11.007
12. Chang JW, Ramchandra R. The sympathetic nervous system in heart failure with preserved ejection fraction. *Heart Fail Rev.* 2025;30:209–218. doi: 10.1007/s10741-024-10456-0

13. Gabisonia K, Khan M, Recchia FA. Extracellular vesicle-mediated bidirectional communication between heart and other organs. *Am J Physiol Heart Circ Physiol*. 2022;322:H769–H784. doi: 10.1152/ajpheart.00659.2021
14. Welsh JA, Goberdhan DCI, O'Driscoll L, Buzas EI, Blenkiron C, Bussolati B, Cai H, Di Vizio D, Driedonks TAP, Erdbrügger U, et al; MISEV Consortium. Minimal information for studies of extracellular vesicles (MISEV2023): from basic to advanced approaches. *J Extracell Vesicles*. 2024;13:e12404. doi: 10.1002/jev2.12404
15. Dworak M, Stebbing M, Kompa AR, Rana I, Krum H, Badoer E. Attenuation of microglial and neuronal activation in the brain by ICV minocycline following myocardial infarction. *Auton Neurosci*. 2014;185:43–50. doi: 10.1016/j.autneu.2014.03.007
16. Tian C, Gao L, Rudebush TL, Yu L, Zucker IH. Extracellular vesicles regulate sympatho-excitation by Nrf2 in heart failure. *Circ Res*. 2022;131:687–700. doi: 10.1161/CIRCRESAHA.122.320916
17. Folick A, Koliwad SK, Valdearcos M. Microglial lipid biology in the hypothalamic regulation of metabolic homeostasis. *Front Endocrinol (Lausanne)*. 2021;12:668396. doi: 10.3389/fendo.2021.668396
18. Frank MG, Fonken LK, Watkins LR, Maier SF. Microglia: neuroimmune-sensors of stress. *Semin Cell Dev Biol*. 2019;94:176–185. doi: 10.1016/j.semcdb.2019.01.001
19. Zhang W, Tian T, Gong SX, Huang WQ, Zhou QY, Wang AP, Tian Y. Microglia-associated neuroinflammation is a potential therapeutic target for ischemic stroke. *Neural Regen Res*. 2021;16:6–11. doi: 10.4103/1673-5374.286954
20. Kim JD, Copperi F, Diano S. Microglia in central control of metabolism. *Physiology (Bethesda)*. 2024;39:0–13. doi: 10.1152/physiol.00021.2023
21. Wang S, Luo Q, Chen H, Huang J, Li X, Wu L, Li B, Wang Z, Zhao D, Jiang H. Light emitting diode therapy protects against myocardial ischemia/reperfusion injury through mitigating neuroinflammation. *Oxid Med Cell Longev*. 2020;2020:9343160. doi: 10.1155/2020/9343160
22. Wang M, Zhang J, Yin Z, Ding W, Zhao M, Liu J, Xu Y, Xu S, Pan W, Wei C, et al. Microglia-mediated neuroimmune response regulates cardiac remodeling after myocardial infarction. *J Am Heart Assoc*. 2023;12:e029053. doi: 10.1161/JAHA.122.029053
23. Lo J, Melhorn SJ, Kee S, Olerich KLW, Huang A, Yeum D, Beiser A, Seshadri S, DeCarli C, Schur EA. Hypothalamic gliosis is associated with multiple cardiovascular disease risk factors in the Framingham heart study. *J Am Heart Assoc*. 2025;14:e039463. doi: 10.1161/JAHA.124.039463
24. Han J, Harris RA, Zhang XM. An updated assessment of microglia depletion: current concepts and future directions. *Mol Brain*. 2017;10:25–25. doi: 10.1186/s13041-017-0307-x
25. Sewaybricker LE, Huang A, Chandrasekaran S, Melhorn SJ, Schur EA. The significance of hypothalamic inflammation and gliosis for the pathogenesis of obesity in humans. *Endocr Rev*. 2023;44:281–296. doi: 10.1210/endrev/bnac023
26. Colombo M, Raposo G, Théry C. Biogenesis, secretion, and intercellular interactions of exosomes and other extracellular vesicles. *Annu Rev Cell Dev Biol*. 2014;30:255–289. doi: 10.1146/annurev-cellbio-101512-122326
27. Li F, Fang R, Rao L, Meng F, Zhao X. [Research progress on exosomes in diagnosis and treatment of cardiovascular diseases]. *Zhejiang da xue xue bao Yi xue ban*. 2018;47:320–326. doi: 10.3785/j.issn.1008-9292.2018.06.17
28. Gan L, Liu D, Xie D, Bond Lau W, Liu J, Christopher TA, Lopez B, Liu L, Hu H, Yao P, et al. Ischemic heart-derived small extracellular vesicles impair adipocyte function. *Circ Res*. 2022;130:48–66. doi: 10.1161/CIRCRESAHA.121.320157
29. Han C, Yang J, Sun J, Qin G. Extracellular vesicles in cardiovascular disease: biological functions and therapeutic implications. *Pharmacol Ther*. 2022;233:108025. doi: 10.1016/j.pharmthera.2021.108025
30. Ottaviani L, Juni RP, de Abreu RC, Sansonetti M, Sampaio-Pinto V, Halkein J, Hegenbarth JC, Ring N, Knoops K, Kocken JMM, et al. Intercellular transfer of miR-200c-3p impairs the angiogenic capacity of cardiac endothelial cells. *Mol Ther*. 2022;30:2257–2273. doi: 10.1016/j.ymthe.2022.03.002
31. Koide T, Mandai S, Kitaoka R, Matsuki H, Chiga M, Yamamoto K, Yoshioka K, Yagi Y, Suzuki S, Fujiki T, et al. Circulating extracellular vesicle-propagated microRNA signature as a vascular calcification factor in chronic kidney disease. *Circ Res*. 2023;132:415–431. doi: 10.1161/CIRCRESAHA.122.321939
32. Doehner W, Ural D, Haeusler KG, Čelutkienė J, Bestetti R, Cavusoglu Y, Peña-Duque MA, Glavas D, Iacoviello M, Laufs U, et al. Heart and brain interaction in patients with heart failure: overview and proposal for a taxonomy. A position paper from the Study Group on Heart and Brain Interaction of the Heart Failure Association. *Eur J Heart Fail*. 2018;20:199–215. doi: 10.1002/ejhf.1100
33. Chen Z, Venkat P, Seyfried D, Chopp M, Yan T, Chen J. Brain-heart interaction: cardiac complications after stroke. *Circ Res*. 2017;121:451–468. doi: 10.1161/CIRCRESAHA.117.311170
34. Cyr B, Cabrera Ranaldi EDLRM, Hadad R, Dietrich WD, Keane RW, de Rivero Vaccari JP. Extracellular vesicles mediate inflammasome signaling in the brain and heart of Alzheimer's disease mice. *Front Mol Neurosci*. 2024;17:1369781. doi: 10.3389/fnmol.2024.1369781
35. Gelosa P, Castiglioni L, Rzemieniec J, Muluhie M, Camera M, Sironi L. Cerebral derailment after myocardial infarct: mechanisms and effects of the signaling from the ischemic heart to brain. *J Mol Med (Berl)*. 2022;100:23–41. doi: 10.1007/s00109-021-02154-3
36. Valadi H, Ekström K, Bossios A, Sjöstrand M, Lee JJ, Lötvall JO. Exosome-mediated transfer of mRNAs and microRNAs is a novel mechanism of genetic exchange between cells. *Nat Cell Biol*. 2007;9:654–659. doi: 10.1038/ncb1596
37. Moldovan L, Batte K, Wang Y, Wisler J, Piper M. Analyzing the circulating microRNAs in exosomes/extracellular vesicles from serum or plasma by qRT-PCR. *Methods Mol Biol*. 2013;1024:129–145. doi: 10.1007/978-1-62703-453-1_10
38. Hoppstädter J, Ammit AJ. Role of dual-specificity phosphatase 1 in glucocorticoid-driven anti-inflammatory responses. *Front Immunol*. 2019;10:1446. doi: 10.3389/fimmu.2019.01446
39. Shi L, Zha H, Pan Z, Wang J, Xia Y, Li H, Huang H, Yue R, Song Z, Zhu J. DUSP1 protects against ischemic acute kidney injury through stabilizing mtDNA via interaction with JNK. *Cell Death Dis*. 2023;14:724. doi: 10.1038/s41419-023-06247-4
40. Wang YC, Koay YC, Pan C, Zhou Z, Tang W, Wilcox J, Li XS, Zagouras A, Marques F, Allayee H, et al. Indole-3-propionic acid protects against heart failure with preserved ejection fraction. *Circ Res*. 2024;134:371–389. doi: 10.1161/CIRCRESAHA.123.322381
41. Zhan J, Jin K, Xie R, Fan J, Tang Y, Chen C, Li H, Wang DW. AGO2 protects against diabetic cardiomyopathy by activating mitochondrial gene translation. *Circulation*. 2024;149:1102–1120. doi: 10.1161/CIRCULATIONAHA.123.065546
42. Dougherty JP, Springer DA, Gershengorn MC. The treadmill fatigue test: a simple, high-throughput assay of fatigue-like behavior for the mouse. *J Vis Exp*. 2016;54052. doi: 10.3791/54052